J | P | S | T

http://jpst.irost.ir

Journal of Particle Science and Technology

IROST

Effect of process parameters on quality properties and drying time of hawthorn in a vibro-fluidized bed dryer

Elham Farzan, Mahmood Reza Rahimi, Vahid Madadi Avargani*

[1] *Department of Chemical Engineering, Yasouj University, Yasouj, Iran*

HIGHLIGHTS

- The kinetic drying of hawthorn in a fluidized bed dryer with and without vibration was studied.
- Effect of vibration intensity, drying air temperature and flow rate on drying rate and shrinkage of hawthorn was investigated.
- All the drying process occurred in the falling rate period and no constant rate period was observed in the drying of hawthorn.
- The vibration intensity, drying air temperatures and flow rate had no significant effect on the shrinkage of hawthorn but has a significant effect on its drying rate.
- The shrinkage varies linearly with respect to moisture content, and the reduction in radial dimension of hawthorn samples was around 40% at the end of the drying process.

ARTICLE INFO

Article history:
Received 16 January 2017
Revised 13 June 2017
Accepted 16 August 2017

Keywords:
Vibro-fluidized bed dryer
Hawthorn drying
Shrinkage
Drying rate
Mathematical modelling

GRAPHICAL ABSTRACT

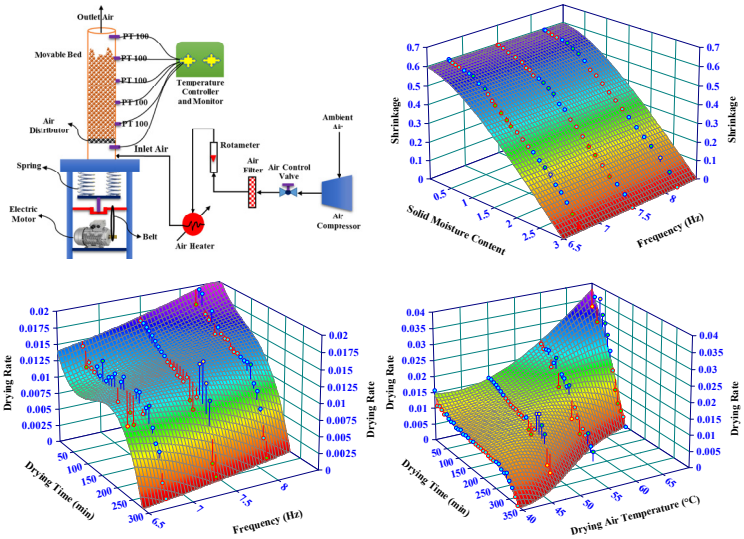

ABSTRACT

The drying kinetics of hawthorn in a pilot-scale experimental fluidized bed dryer with and without vibration was investigated. The effect of operating parameters, such as vibration intensity, drying air flow rate, and temperature, on the drying rate and shrinkage of hawthorn was studied. The hawthorn fruit was dried at various drying air temperatures ranging from 40-70°C and drying air volume flow rates ranging from 22-30 m^3/h with the vibration intensity ranging from 6.8 to 8.2 Hz. The entire drying process occurred in the falling rate period and no constant rate period was observed in the drying of hawthorn. Four mathematical drying models investigating the drying behavior of hawthorn were evaluated and then the experimental moisture data were fitted in these models. The quality of the models fitting was assessed using the coefficient of determination, chi-square and root mean square error. The logarithmic and Page models for drying rate and the Ratti and Vazquez models for shrinkage were found to be the most suitable for describing the drying and shrinkage curves of hawthorn. The results showed that the vibration intensity, drying air temperature and flow rate has no significant effect on the shrinkage of hawthorn. All mentioned parameters had a significant effect on the drying rate of hawthorn, but the effect of drying air temperature was considerably more compared to the other parameters. It was observed that shrinkage varies linearly with respect to moisture content, and the reduction in radial dimension of hawthorn samples was around 40% at the end of the drying process.

* *Corresponding author. Tel.: +9874-31005064 ; Fax: +9874-31009555 ; E-mail address: v.madadi@yu.ac.ir*
DOI: 10.22104/JPST.2017.1918.1065

1. Introduction

Agricultural products are often initially relatively high in moisture content and are highly vulnerable to pollution and corruption. Spoilage is variable depending on the type of material, and products can be rendered completely unusable in a short period of time. Therefore, the drying of agricultural product is very important and a variety of dryers can be used. In the drying process the method of drying greatly effects the product quality by reducing the moisture content to an acceptable level and extending the shelf life of products [1,2].

There are many different drying techniques and procedures used to reduce water from foodstuffs and increase the shelf life of these food materials. Convective drying is the most generally employed method due to its simplicity and cost effectiveness. Fluidized bed dryers are widely used in drying processes, especially in the food industry, because of their drying uniformity, relative low cost of operation and high rate of drying [3].

Nowadays, Vibro-Fluidized Bed Dryers (V-FBD) are highly regarded in food drying processes since they have greater efficiency than conventional types of fluidized bed dryers. V-FBDs can be used as a strategy to improve the fluidization quality of materials [4], increase the bed uniformity as a result of using vibration in the fluidized beds, and to avoid some problems like channeling and de-fluidization, all which improve drying of materials in fluidized bed dryers. The vibrating fluidized bed dryer is a modification of a common fluidized bed dryer, in which the vibration energy is used to transfer the material from a packed to fluidized state. Vibration can be produced by mechanical shaking of the entire apparatus [5,6].

One of the most important physical changes commonly seen in the early stages of material drying is a reduction in the size of the material's outer shell also called shrinkage [7,8]. Fruits are porous in nature and can experience shrinkage during the drying processes, which can affect the drying time. This shrinkage can be controlled in V-FBDs by various parameters such as intake air temperature and velocity and frequency of the engine device [9]. Fruits have high initial moisture content, and due to evaporation of the moisture contained in the fruit the shrinkage phenomenon is an undesirable change that can occur during drying. The shrinkage of material can affect the mass transfer diffusion coefficient in the drying process and consequently the drying time and rate [7,10-12]. Also, from the food industry standpoint, shrinkage can affect the quality of food drying. The amount of shrinkage is different for each material and depends on the initial moisture content and the structure of the material. The material shrinkage can be controlled by several operational and structural parameters in drying processes such as inlet air temperature and velocity and frequency of the bed in a V-FBD [8,13,14].

Marring et al. studied the effect of vibration on a fluidized bed dryer for potato starch drying and observed that potato starch, which did not fluidize with aeration alone, could become well fluidized when vibration was applied [15]. Jinescu et al. reported that the vibrational state of the bed allows an increase in the drying rate due to the consequent increase in the specific area of gas–solid contact [16]. Karbassi et al. reported that bed uniformity, as a result of using vibration in fluid beds, can be achieved by preventing bubbles in the bed [17]. Also, the vibration helps to overcome interparticle forces, consequently improving the fluidization of material [18]. Mori et al. studied the drying behavior of sawdust particles in a vibro-fluidized bed dryer and found that using a vibro-fluidized dryer significantly reduced the required air velocity for drying sawdust [19].

Sadeghi and Khoshtaghaza studied the drying behavior of tea particles in vibro-fluidized bed dryers and found that the vibration system decreases the minimum fluidization velocity of tea particles in the bed, and this velocity was reduced by increasing the vibration intensity [20]. Lima and Ferreira examined fluidized and vibro-fluidized shallow beds for drying fresh leaves and concluded that the MCB dryer with vibration to produce a convenient configuration of drying can be used [21]. Silva Costa et al. analyzed the use of a hybrid CSTR/neural network model to describe the highly coupled heat and mass transfer during paste drying with inert particles in vibro-fluidized beds. The dynamics behavior of the outlet air temperature and relative humidity are described well by the CSTR lumped model for most evaluated conditions [22].

Nunes et al. investigated the fluid dynamics and polymeric coating of sodium bicarbonate in a vibro fluidized bed. In all experimental conditions there was an improvement in sodium bicarbonate fluidization, and a reduction in clusters and preferential channels compared to CFB [23]. Fyhr and Kemp presented a

multiparticle model for fluidized bed dryers to study two different materials (zeolite and wheat), and the model predictions showed a good agreement with experimental data. Moreover, the calculations showed that the model can be used for transient conditions as well [24].

Zanoelo considered a theoretical and experimental study of simultaneous heat and mass transport resistances in a shallow fluidized bed dryer of mate leaves. An analysis of the joint confidence regions of both external heat and effective mass transfer coefficients was carried out and a significant effect of the equivalent particle diameter and temperature on these model parameters was observed [25].

The aim of this present work is to investigate the effect of some parameters such as vibration intensity, drying air temperature and flow rate on the shrinkage, drying time and drying kinetics of hawthorn in a fluidized bed dryer with and without vibration. In addition, the experimental moisture data is fitted to various mathematical models available from the literature.

2. Materials and methods

2.1. Hawthorn samples preparation

In this work, which is designed to dry hawthorn in a fluidized bed dryer, the fresh hawthorn samples were picked from a local tree at Yasouj University, situated in south-west Iran. The hawthorn samples were stored in a refrigerator for 24 h at 4±1°C. The weight of the samples was determined by means of an electronic balance (AND model GF600, Japan) with an accuracy of 0.001 g. A photo of the hawthorn samples used in the experiment is shown in Figure 1. Based on device capacity and fundamentals of the drying process, the operating range of the study parameters are found in Table 1. According to the design of experiments (DOEs) in Design Expert Software, the number of optimized experiments and the magnitude of study parameters were obtained and are given in Table 2. The weight of three hawthorn fruit samples and the averaged dimensions of the dried samples in three directions were measured by means of a sliding gauge at different time intervals during each run. Experiments to determine the influence of process variables on shrinkage and drying time of hawthorn in a fluidized bed dryer with and without vibration were performed. The average diameter and

Fig. 1. Photo of hawthorn samples used in the experiments

Table 1. The operating range of considered parameters in the fluidized bed dryer

Variable	Symbol	Operating Range
Inlet air temperature (°C)	T	40-70
Ambient air temperature (°C)	T_a	28 ± 2
Ambient air relative humidity (%)	RH	27 ± 3
Air flow rate (m^3/h)	Q	22-30
Frequency (Hz)	f	6.8-8.2

the shrinkage of samples in the experiments are given by Eqs. (1) and (2), respectively, as below [26-28]:

$$D = \sqrt[3]{ABC} \tag{1}$$

$$Sh = (1 - \frac{D_t}{D_0}) \times 100 \tag{2}$$

where, the parameters A, B and C in Eq. (1) are the dimensions of the dried samples in three directions, and D_t and D_0 in Eq. (2) are the instant and initial diameter of the samples, respectively.

2.2. Drying apparatus

A pilot-scale vibro-fluidized bed dryer was set up for performing the drying experiments. The schematic diagram of the experimental apparatus is shown in Figure 2. The dryer is made of a plexiglass column with a 0.1 m inside diameter, a height of 0.8 m, and a fitted perforated metal plate at the bottom as an air distributor. Drying air is supplied from a high-pressure air compressor and its pressure is adjusted by a regulator. The air is then passed through a rotameter before entering an electrical heater to raise the temperature of the drying air. Six PT100 thermocouples are used to measuring the air temperature along the bed length and

Table 2. Experimental design of hawthorn drying process in the fluidized bed dryer Experiment

#	Repetitions	Inlet air temperature (°C)	Air flow rate (m^3/h)	Frequency (Hz)	Amount of sample (gr)
1	1	40	24	7.15	250
2	1	50	22	7.50	250
3	3	50	26	7.50	250
4	1	60	28	7.85	250
5	1	60	24	7.15	250
6	1	30	26	7.50	250
7	1	60	26	7.15	250
8	1	50	26	8.20	250
9	1	40	28	7.15	250
10	1	50	26	6.80	250
11	1	70	26	7.50	250
12	1	60	24	7.85	250
13	1	50	30	7.50	250
14	1	40	24	7.85	250
15	1	40	28	7.85	250

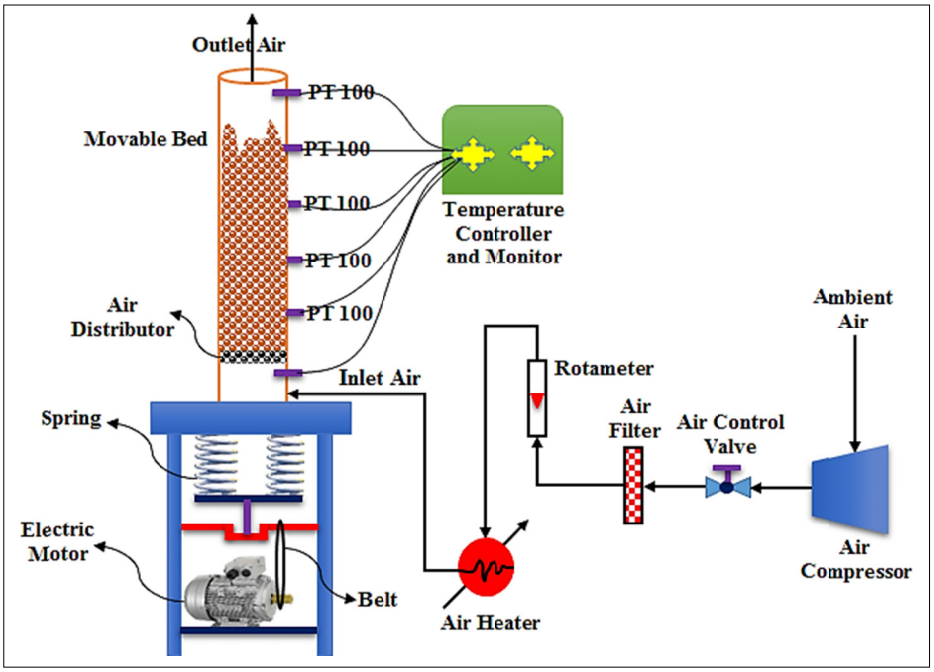

Fig. 2. Schematic diagram of the pilot plant vibro-fluidized bed dryer

a temperature controller with a temperature indicator is used for regulating and showing the temperatures of the drying air medium entering the bed within ±2°C. The inlet and outlet air temperature, velocity and humidity are measured by means of an electronic temperature/ humidity meter (Model Testo 480, Germany, with a vane measurement probe of Ø 3.9" and a humidity and temperature probe of Ø 0.5", see Figure 3). The sample moisture (on a dry basis) was determined by measuring the wet and dry weight of the sample and using Eq. (3) as below:

$$\frac{w_w \quad w_d}{} \tag{3}$$

where, M_d is the solid moisture content on a dry basis, and W_w and W_d are the wet and dry weight of solid samples, respectively.

The bed was vibrated through movement of the entire bed. To operate in the vibro-fluidized mode, the displacement was controlled by an electric motor with variable rotation, an eccentric mechanism was used to adjust the amplitude of vibration, and a mechanical

Fig. 3. The device which is used to measure air humidity, temperature and velocity

controller using a belt and two springs located at the axle of the electric motor allowed for adjustment of the vibration frequency as shown in Figure 2.

3. Mathematical modelling

Four simplified drying models, given in Table 3, have been used to describe the drying kinetics of hawthorn. Four simplified shrinkage models, given in Table 4, have been used to describe the shrinkage of hawthorn in the present work.

In these models, *MR* represents the dimensionless moisture ratio and can be given by the following equation:

$$MR = \frac{M_t}{M_0} \tag{4}$$

where, M_t is the moisture content at time t, and M_0 is the initial moisture content. A non-linear regression analysis was performed using TableCurve 3D software (Version 4.0) to fit the selected mathematical models with the experimental data. The coefficient of determination, R^2, is one of the primary criteria in order to evaluate the fit quality of these models. In addition, the reduced chi-square (χ^2) and root mean square error (*RMSE*) were used to determine suitability of the fit. The coefficient of determination and reduced chi-square and RMSE can be calculated as follows:

$$R^2 = 1 - \frac{\sum_{i=1}^{N}\left(P_{pred,i} - P_{\exp,i}\right)^2}{\sum_{i=1}^{N}\left(\overline{P}_{pred.i} - P_{\exp,i}\right)^2} \tag{5}$$

$$\chi^2 = \frac{\sum_{i=1}^{N}\left(P_{\exp.i} - P_{pred,i}\right)^2}{N - Z} \tag{6}$$

Table 3. Mathematical models applied to drying curves

No.	Model name	Model
1	Newton [1]	$MR = \exp(-Kt)$
2	Page [2]	$MR = \exp(-Kt)^n$
3	Henderson and Pabis [3]	$MR = a\exp(-Kt)$
4	Logarithmic [4]	$MR = a\exp(-Kt) + C$

Table 4. Mathematical models applied to shrinkage curves

No.	Model name	Model
1	Mayor and Sereno [5]	$Sh = k_1 + k_2(MR) + k_3(MR)^2$
2	Ratti [6]	$Sh = k_4 + k_5 M_t + k_6 M_t^{\,2} + k_7 M_t^{\,3}$
3	Mulet *et al.* [5]	$Sh = k_8 + k_9\left(\frac{M_t}{1+M_t}\right) + \exp\left(k_{10}\frac{M_t}{1+M_t}\right)$
4	Vazquez *et al.* [7]	$Sh = k_{11} + k_{12}M_t + k_{13}M_t^{\,3/2} + k_{14}\exp(k_{15}M_t)$

$$RMSE = \sqrt{\frac{\left(\sum_{i=1}^{N}\left(P_{\exp,i} - P_{pred,i}\right)^2\right)}{N}} \tag{7}$$

where, $P_{exp,i}$ is the i^{th} experimental data such as the moisture ratio ($MR_{exp,i}$) and shrinkage ($Sh_{exp,i}$), $P_{pred,i}$ is the i^{th} predicted value, N is the number of observations and Z is the number of constants in a model. The higher the R^2 values and lower the (χ^2) and *RMSE* values, the better the goodness of fit [29-32].

4. Results and discussions

4.1. Analysis of drying curves

Several drying experiments were carried out under different operating conditions to investigate the effect of operating parameters, such as drying air flow rate and temperature, on shrinkage and drying time of hawthorn with and without vibration in a fluidized bed. The changes in diameter of the drying sample and the weight of test samples were determined, and consequently the shrinkage and moisture content of the samples were estimated. The drying curves [*MR=MR(t)*] of the hawthorn dried in a fluidized bed dryer with and without vibration for different values of drying air temperature and flow rate are as shown in Figures 4-6. As it is seen from these figures, the moisture content decreases continuously with drying time. The vibration

intensity, the drying air temperature and flow rate have a significant effect on the drying kinetics of hawthorn. Increasing vibration intensity, drying air temperature and flow rate reduced the drying time of the hawthorn, and the drying air temperature had the most significant effect on this reduction. The shortest drying time in the experiments was observed for the V-FBD with the greatest vibration intensity (f=8.2 Hz) and a drying air temperature equal to 70°C.

Figure 4 shows the effect of drying air flow rate on the drying time of hawthorn in a fluidized bed dryer with and without vibration. As can be seen, drying time decreases as drying air flow rate increases due to increases in the convective heat and mass transfer coefficients. The variation of moisture ratio versus drying time for different drying air temperatures is shown in Figure 5. The drying air temperature had a more significant effect on drying time compared to the drying air flow rate and vibration intensity. The driving force for heat transfer from the gas phase to solid particle is the difference between the gas and solid temperatures, which causes moisture to be transferred from a solid particle to the gas phase. By increasing drying air temperature, the heat and mass transfer increase; hence, the drying time is significantly decreased. When the drying air temperature increased from 40 to 70°C, the drying time decreased about 60%. Figure 6 shows the effect of vibration intensity on drying time of hawthorn in the bed. The results show that an increase of about 20% in the vibration intensity decreased the drying time about 20%. This can be explained by an increase in the gas-solid contact area due to the prevention of particles sticking to each other, and as a result increases the heat and mass transfer between the gas phase and solid particles. Similar results have been reported by previous researchers [16,33].

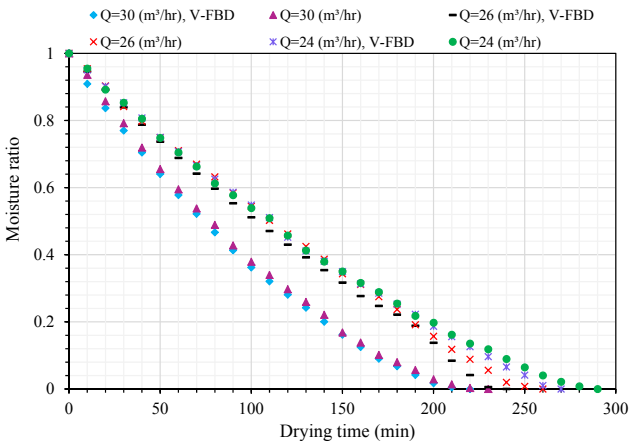

Fig. 4. Moisture ratio versus drying time of hawthorn at different drying air flow rates (drying air temperature=50°C and vibration intensity=7.5 Hz in vibro mode)

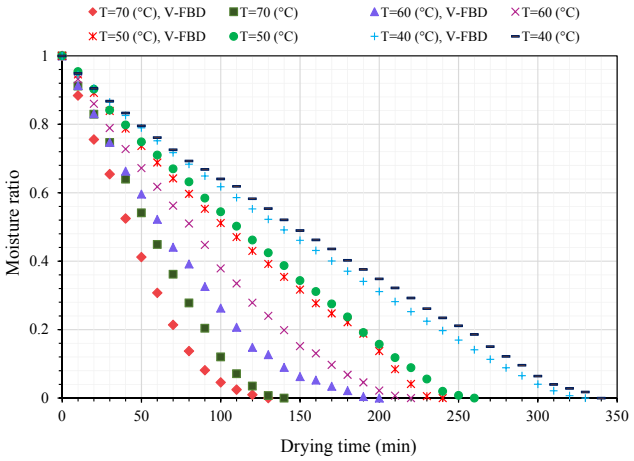

Fig. 5. Moisture ratio versus drying time of hawthorn at different drying air temperatures (drying air flow rate=26 m³/h and vibration intensity=7.5 Hz in vibro mode)

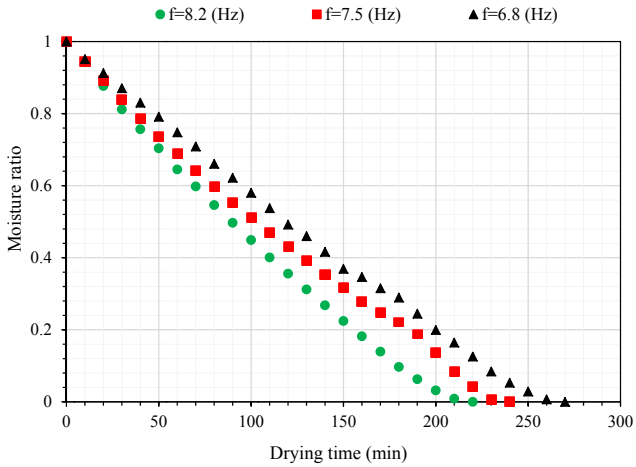

Fig. 6. Moisture ratio versus drying time of hawthorn at different vibration intensity (drying air flow rate=26 m³/h and drying air temperature=50°C)

4.2. Analysis of shrinkage curves

Variation of hawthorn shrinkage during drying time with and without vibration at different drying air temperature is shown in Figure 7. The results show that the vibration intensity has no significant effect on the shrinkage of hawthorn. Figure 7 also shows that the effect of drying air temperature on drying time is more significant compared to vibration intensity. When the drying air temperature increased, the drying time decreased significantly and at the end of the drying process the amount of hawthorn shrinkage is the same for various drying air temperatures with and without

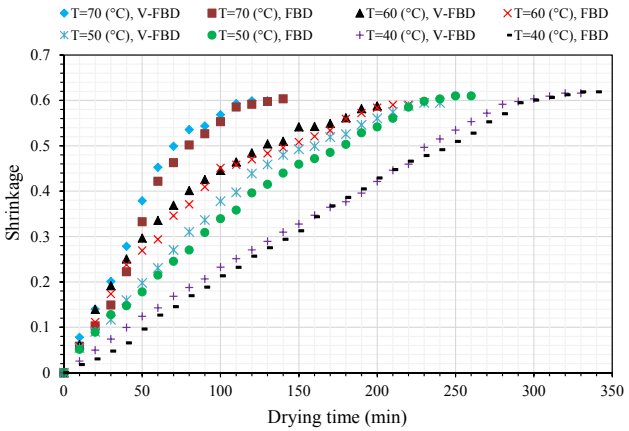

Fig. 7. Shrinkage variation versus drying time of hawthorn at drying air temperatures with and without vibration (drying airflow rate= 26 m^3/h)

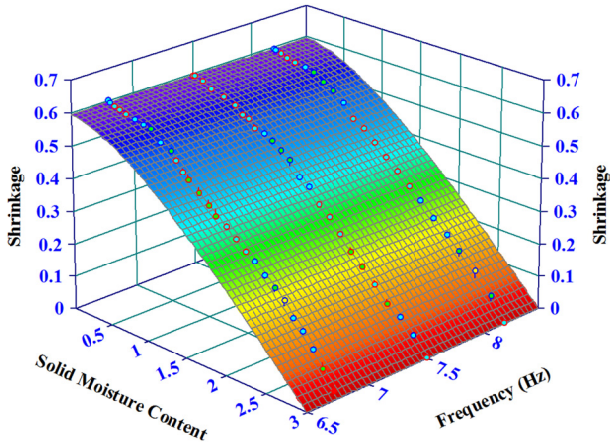

Fig. 8. Variation of hawthorn shrinkage versus solid moisture content at different vibration intensity (drying air flow rate=26 m^3/h and drying air temperature=50°C)

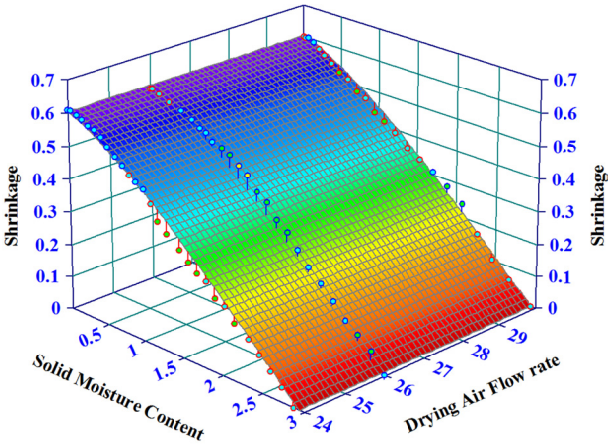

Fig. 9. Variation of hawthorn shrinkage versus solid moisture content at different drying air flow rates (vibration intensity=7.5 Hz and drying air temperature=50°C)

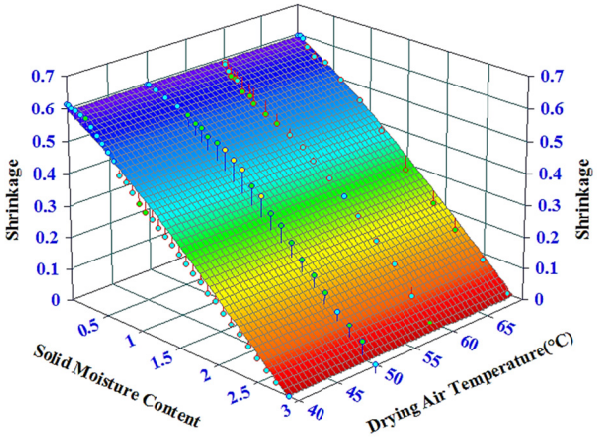

Fig. 10. Variation of hawthorn shrinkage versus solid moisture content at different drying air temperatures (drying air flow rate=26 m^3/h and vibration intensity=7.5 Hz)

For more clarity, other types of 3D graphs which investigate the effect of the studied parameters on shrinkage and drying rate are reported. The effect of solid moisture content, drying air flow rate and temperature on shrinkage of hawthorn dried in the fluidized bed dryer with and without vibration are shown in Figures 8-10. According to the results shown in these figures, the vibration intensity, drying air temperature and flow rate have no considerable effect on shrinkage of hawthorn in the fluidized bed dryer. Figures 8-10 show that at the end of the process when the solid moisture content is at its minimum value, the amount of shrinkage is at its maximum value. Although the solid moisture content and consequently the drying rate vary for different drying air conditions and various vibration intensities, the amount of shrinkage for various vibration intensities, drying air temperatures and flow rates remains the same for a constant solid moisture content. While the rate of shrinkage for higher drying air temperatures is greater than lower temperatures, at the end of the process the amount of the shrinkage is the same for all drying temperatures. According to Figure 8, when the solid moisture has a specified value the amount of shrinkage is the same, even for various bed vibration intensities.

The shrinkage profile of hawthorn with respect to solid moisture content for various studying parameters are shown in Figures 8-10. They clearly depict that shrinkage of the sample occurs almost linearly with solid moisture content, or in the other words, with drying time. Sometimes due to severe drying conditions, rapid shrinkage of sample surface occurs which leads to cracking of the surface. Surface cracking due to non-uniform shrinkage leads to the formation of unbalanced stresses and failure of the material. In this study, results show that the shrinkage of hawthorn in the fluidized bed dryer with and without vibration is approximately

uniform, and as a result the surface cracking phenomenon does not occur.

In addition, Figures 8-10 show that up to 60% shrinkage was observed in the hawthorn sample during the entire process. Conversely, the diameter of the hawthorn sample only reduced to 40% of its original diameter at the end of the drying process.

4.3. Analysis of drying rate curves

The drying rate (*DR*) is defined as the amount of the evaporated moisture from the solid body over drying time. The drying rates of hawthorn were calculated by the following equation [2]:

$$DR = \frac{M_{t+dt} - M_t}{t} \tag{8}$$

where, M_{t+dt} and M_t are the solid moisture content at time t and $t+dt$, respectively, based on a dry solid basis (kg water/ kg dry solid) and t is the drying time (min).

Figures 11-15 show the variation of drying rate for hawthorn in a fluidized bed dryer with and without vibration versus drying time at different vibration intensities, drying air temperatures and flow rates. The results in these figures show that the drying rate decreases continuously with drying time due to a reduction in solid moisture content. The drying rate curves show that there was no constant drying period during the drying of hawthorn. All of the drying rate curves show that the drying of hawthorn occurs in the falling rate period; solid internal molecular diffusion is the dominant mechanism in this period of drying. Some similar results were reported in previous works for other agricultural products such as olive pomace [2, 34-36], organic tomatoes [37], green peppers [38], and figs [39].

The results in Figures 11-13 indicate that the drying rate in a fluidized bed with vibration is greater than the drying rate without vibration. As mentioned before, when vibration is applied to the dryer the efficiency of gas-solid contact increases because the particles are prevented from sticking to each other and the minimum fluidization velocity and fluidization pressure drops decrease and homogeneity and stability of the fluidized bed layers increase. Finally, as a result, the heat and mass transfer between the gas phase and solid particles, and consequently the drying rate increases in the vibro-fluidized bed mode. The results in Figure 13 indicate that increasing the vibration intensity from 6.8 to 8.2 Hz for a drying air temperature and flow rate equal to 50°C and 26 m³/h, respectively, reduced the drying time by about 20%. In addition, at the beginning of the process, when

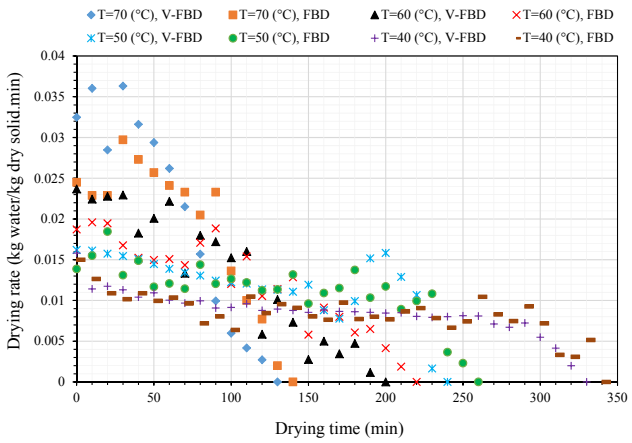

Fig. 11. Drying rate versus drying time at different drying air temperatures with and without vibration (drying air flow rate=26 m³/h, vibration intensity=7.5 Hz)

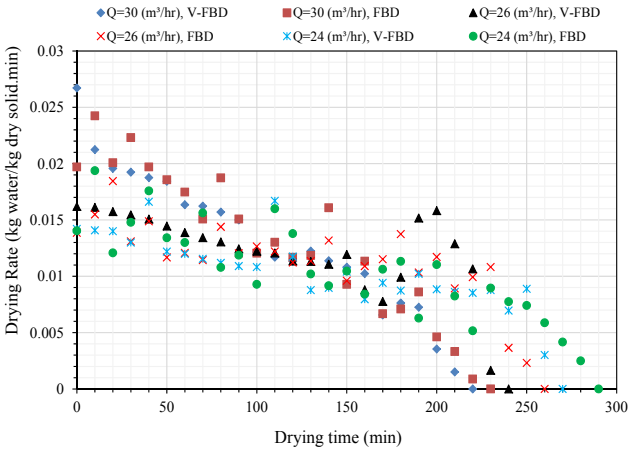

Fig. 12. Drying rate versus moisture content at different drying air flow rates with and without vibration (drying air temperature=50°C, vibration intensity=7.5 Hz)

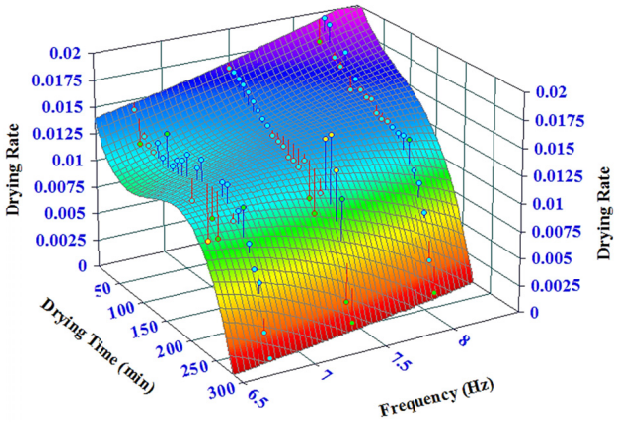

Fig. 13. Drying rate versus drying time of hawthorn at different vibration intensity (drying air flow rate=26 m³/h and drying air temperature=50°C)

the solid moisture content is high, the drying rate for vibration intensity equal to 8.2 Hz is about 33% greater than when the vibration intensity is equal to 6.8 Hz.

The effect of drying air flow rate on the drying rate of hawthorn in a fluidized bed dryer with and without vibration is illustrated in Figures 12 and 14. The results show that by increasing the drying air flow rate the drying rate increases, and consequently the drying time decreases. This can be explained as when the drying air flow rate increases the convective heat and mass transfer coefficient increase and the amount of heat transfer from the gas phase to the solid phase and the moisture transfer from the solid phase to the gas phase increase. The results in Figure 14 show that when drying air temperature and vibration intensity are equal to 50°C and 7.5 Hz, respectively, increasing the drying air flow rate from 26 to 30 m^3/h reduces the drying time of hawthorn about 20%.

One of the most important operating parameters in the drying process is the drying air temperature. In the drying of materials, the drying air temperature is selected based on many essential factors such as the thermal properties of the materials and the desired quality of the dried materials. In food industries, this is more important than other operating parameters. In this study, a range of 40 to 70°C was selected for the experiments. In drying processes with warm air, the moisture is transfer from the solid body to the solid surface and then to the gas phase by heat transfer from the gas phase to the solid surface. Therefore, in a drying process with warm air, the convective heat transfer is a function of the convective heat transfer coefficient and the difference between the solid-gas interface and gas bulk temperatures.

The effect of drying air temperature on the drying rate and consequently drying time of hawthorn in the fluidized bed dryer with and without vibration is shown in Figures 11 and 15. It can be seen from these figures that the drying air temperature had a more significant effect on the drying time of hawthorn in the fluidized bed compared to the drying air flow rate and vibration intensity. According to the results in Figure 15, increasing the drying air temperature from 40 to 70°C decreases the drying time about 60%.

4.4. Models of drying and shrinkage curves

The amount of hawthorn shrinkage and moisture ratio at different times were measured by the methods mentioned above. The obtained experimental data from the drying of hawthorn in the fluidized bed dryer for various conditions were fitted to four mathematical models listed in Tables 1 and 2 for moisture ratio and hawthorn shrinkage, respectively. Values of the determination coefficient (R^2), the reduced chi-square (χ^2) and the root mean square error (*RMSE*) for different drying air temperatures determined by non-linear regression analysis are necessary to suggest a proper equation to predict the suitable behavior of hawthorn drying in a fluidized bed dryer, see Tables 5 and 6. In accordance with the results shown in these tables, the R^2, χ^2 and *RMSE* values for the moisture ratio ranges from 0.950462 to 0.999370, 0.000072 to 0.004009 and 0.007881 to 0.079668, respectively. The R^2, χ^2 and *RMSE* values for shrinkage ranges from 0.824923 to 0.999634, 0.000080 to 0.006971 and 0.008507 to

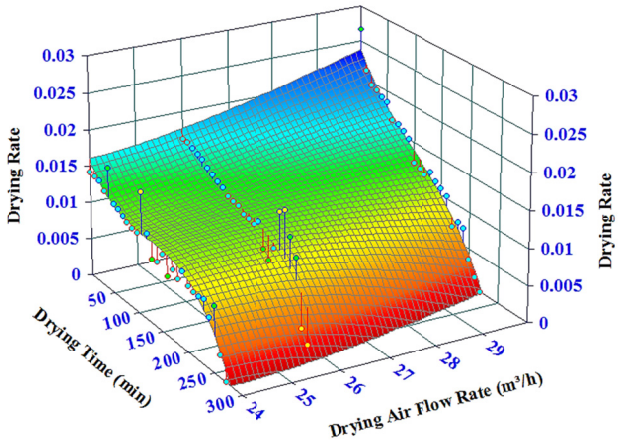

Fig. 14. Drying rate versus drying time of hawthorn at different drying air flow rates (drying air temperature=50°C and vibration intensity=7.5 Hz)

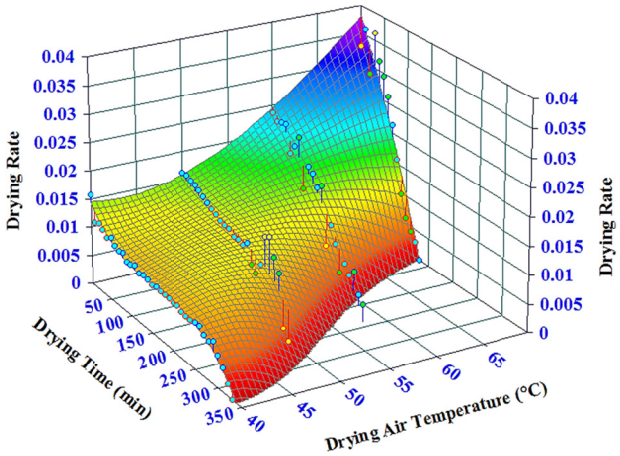

Fig. 15. Drying rate versus drying time of hawthorn at different drying air temperatures (drying air flow rate=26 m^3/h and vibration intensity=7.5 Hz)

Table 5. Statistical results of mathematical models fitting for moisture ratio at different drying air temperatures

Model	T (°C)	R^2	χ^2	*RMSE*
Newton	70	0.956640	0.003824	0.060345
	60	0.962428	0.004009	0.061791
	50	0.966199	0.003643	0.058906
	40	0.950462	0.002845	0.052054
Page	70	0.997413	0.000310	0.016759
	60	0.997086	0.000487	0.021001
	50	0.990251	0.001029	0.030511
	40	0.981352	0.002807	0.050394
Henderson and Pabis	70	0.965764	0.003138	0.053280
	60	0.972556	0.003087	0.052850
	50	0.973009	0.003066	0.052669
	40	0.956158	0.007015	0.079668
Logarithmic	70	0.995653	0.000724	0.024916
	60	0.995563	0.000526	0.021233
	50	0.999370	0.000075	0.008038
	40	0.999339	0.000072	0.007881

Table 6. Statistical results of mathematical models fitting for hawthorn shrinkage at different drying air temperatures

Model	T (°C)	R^2	χ^2	*RMSE*
Mayor and Sereno	70	0.996735	0.000134	0.011308
	60	0.994478	0.000170	0.012741
	50	0.995845	0.000157	0.012234
	40	0.982852	0.002917	0.051239
Ratti	70	0.999434	0.000083	0.008694
	60	0.999634	0.000080	0.008507
	50	0.996822	0.000127	0.010700
	40	0.996951	0.000111	0.010025
Mulet *et al.*	70	0.907306	0.003994	0.060113
	60	0.841852	0.005139	0.068188
	50	0.824923	0.006971	0.079417
	40	0.851827	0.005224	0.068748
Vazquez *et al.*	70	0.997652	0.000107	0.009566
	60	0.992577	0.000255	0.014773
	50	0.996324	0.000158	0.053245
	40	0.998003	0.000090	0.008804

0.079417, respectively. The highest values for the determination coefficient and the lowest values for the reduced chi-square and root mean square error indicate a good fit in all cases.

From the drying curves in the models considered the Page and logarithmic models gave values of R^2 higher than 0.99 for almost all drying air temperatures, except the value of R^2 was 0.981352 in the Page model at a drying air temperature of 40°C. Furthermore, the values of *RMSE* and chi-square for the drying curves in the Page and logarithmic models were less than the two others. The drying curve analysis shows that at higher drying air temperatures the Page model predicted better than the logarithmic and the logarithmic model predicted better at lower temperatures. The logarithmic and Page models appear to be the most appropriate in describing the drying rate of hawthorn under the experimental conditions studied.

Among the models considered for hawthorn shrinkage, Ratti and Vazquez models gave values of R^2 above 0.99 for all drying air temperatures in the range of (40-70°C). The Ratti and Vazquez models gave comparatively higher values for R^2 in all drying air temperatures, whereas χ^2 and *RMSE* values were lower. Thus, these models appear to be the mosappropriate in describing the shrinkage of hawthorn under the experimental conditions studied. Among the others investigated mathematical models, the Newton, Henderson and Pabis models for drying rate and the Mulete model for shrinkage appear to be the least suitable models for the drying and shrinkage behavior of hawthorn under the experimental conditions studied.

5. Conclusions

In this study, the effect of drying air temperature and flow rate ranging from 40 to 70°C and 22 to 30 m^3/h, respectively, on the drying rate and shrinkage of hawthorn in a fluidized bed dryer with and without vibration was investigated. The drying of hawthorn took place only in the falling rate period. Behavior of shrinkage changes along the the drying process was demonstrated and the effect of the mentioned parameters on hawthorn shrinkage was studied. A uniform radial shrinkage, up to 60% of the original radius at the end of drying process, was observed to happen linearly with respect to the solid moisture content. It is observed that the vibration intensity, drying air temperature and flow rate have no significant effect on the shrinkage of hawthorn. The effect of the mentioned parameters on the drying rate of hawthorn was investigated and results show that the drying air temperature has a more significant effect on the drying rate of hawthorn than the other parameters. For drying air flow rate and vibration intensity equal to 26 m^3/h and 7.5 Hz, respectively,

increasing the drying air temperature from 40 to 70°C decreased the drying time by about 60%.

The drying and shrinkage curves were fitted to four different mathematical drying models, and the logarithmic and Page models for drying rate and the Ratti and Vazquez models for shrinkage were found to be the most suitable for describing the drying and shrinkage curves of hawthorn under the experimental conditions studied

Nomenclature

Sh	Shrinkage, (dimensionless)
D_0	Initial diameter of product, (mm)
D_t	Diameter of the dried product, (mm)
W_w	Initial weight of undried product, (gr)
W_d	Weight of dry matter in product, (gr)
M_d	Moisture (on dry basis), (kg water/kg dry solid)
D	Average diameter, (mm)
A, B, C	Three orthogonal diameters, (mm)
MR	Moisture ratio, (dimensionless)
M_t	Moisture content at time t, (kg water/kg dry matter)
M_0	Initial moisture content, (kg water/kg dry matter)
R^2	Coefficient of determination
Z	Number of constants in a model
$P_{pred,i}$	i^{th} predicted value
$P_{exp,i}$	i^{th} experimental value
χ^2	chi-square, (dimensionless)
N	Number of experiments
$RMSE$	Root mean square error, (dimensionless)
k_1-k_{15}	Constants in models, (dimensionless)
a, n, c	Coefficients in models, (dimensionless)
t	Drying time, (min)
T	Drying air temperature, (°C)

References

[1] J. Aprajeeta, R. Gopirajah, C. Anandharamakrishnan, Shrinkage and porosity effects on heat and mass transfer during potato drying, J. Food Eng. 144 (2015) 119-128.

[2] S. Meziane, Drying kinetics of olive pomace in a fluidized bed dryer, Energ. Convers. Manage. 52 (2011) 1644-1649.

[3] I. Białobrzewski, M. Zielińska, A.S. Mujumdar, M. Markowski, Heat and mass transfer during drying of a bed of shrinking particles–Simulation for carrot cubes dried in a spout-fluidized-bed drier, Int. J. Heat Mass Tran. 51 (2008) 4704-4716.

[4] E. Jaraiz, S. Kimura, O. Levenspiel, Vibrating beds of fine particles: estimation of interparticle forces from expansion and pressure drop experiments, Powder Technol. 72 (1992) 23-30.

[5] R. Moreno, R. Rios, H. Calbucura, Batch vibrating fluid bed dryer for sawdust particles: experimental results, Dry. Technol. 18 (2000) 1481-1493.

[6] M. Stakić, T. Urošević, Experimental study and simulation of vibrated fluidized bed drying, Chem. Eng. Process. 50 (2011) 428-437.

[7] M. Prado, Drying of dates (Phoenix Dactyulifera L.) to obtain dried date (passa), Campinas, UNICAMP, 1998.

[8] L. Mayor, A. Sereno, Modelling shrinkage during convective drying of food materials: a review, J. Food Eng. 61(3) (2004) 373-386.

[9] I. Sjöholm, V. Gekas, Apple shrinkage upon drying, J. Food Eng. 25 (1995) 123-130.

[10] N. Wang, J. Brennan, Changes in structure, density and porosity of potato during dehydration, J. Food Eng. 24 (1995) 61-76.

[11] W. Senadeera, B.R. Bhandari, G. Young, B. Wijesinghe, Influence of shapes of selected vegetable materials on drying kinetics during fluidized bed drying, J. Food Eng. 58 (2003) 277-283.

[12] B.A. Souraki, D. Mowla, Axial and radial moisture diffusivity in cylindrical fresh green beans in a fluidized bed dryer with energy carrier: Modeling with and without shrinkage, J. Food Eng. 88 (2008) 9-19.

[13] G. Hashemi, D. Mowla, M. Kazemeini, Moisture diffusivity and shrinkage of broad beans during bulk drying in an inert medium fluidized bed dryer assisted by dielectric heating, J. Food Eng. 92 (2009) 331-338.

[14] E. Marring, A. Hoffmann, L. Janssen, The effect of vibration on the fluidization behaviour of some cohesive powders, Powder Technol. 79 (1994) 1-10.

[15] G. Jinescu, C. Tebrencu, E. Ionescu, M. Petrescu, C. Jinescu, Hydrodynamic aspects at vibrated-fluidized drying of polydisperse powdery materials, in International Drying Symposium IDS2000, 2000.

[16] A. Karbassi, Z. Mehdizadeh, Drying rough rice in a fluidized bed dryer, J. Agr. Sci. Tech.-Iran. 10 (2010) 233-241.

[17] D. Kunii, O. Levenspiel, Fluidization Engineering. Butterworth-Heinemann, Boston, 1991.

[18] S. Mori, Vibro-fluidization of group-c particles and its industrial application, in AIChE Symp. Ser. 1990.
[19] M. Sadeghi, M. Khoshtaghaza, Vibration effect on particle bed aerodynamic behavior and thermal performance of black tea in fluidized bed dryers, J. Agr. Sci. Tech.-Iran. 14 (2012) 781-788.
[20] R.d.A.B. Lima, M. do Carmo Ferreira, Fluidized and vibrofluidized shallow beds of fresh leaves, Particuology 9 (2011) 139-147.
[21] A.S. Costa, F.B. Freire, J. Freire, M. Ferreira, Modelling drying pastes in vibrofluidized bed with inert particles, Chem. Eng. Process. 103 (2016) 1-11.
[22] J.F. Nunes, F.C.A. de Alcântara, V.A. da Silva Moris, S.C. dos Santos Rocha, Fluid dynamics and coating of sodium bicarbonate in a vibrofluidized bed, Chem. Eng. Process. 52 (2012) 34-40.
[23] C. Fyhr, I.C. Kemp, Mathematical modelling of batch and continuous well-mixed fluidised bed dryers, Chem. Eng. Process. 38 (1999) 11-18.
[24] E.F. Zanoelo, A theoretical and experimental study of simultaneous heat and mass transport resistances in a shallow fluidized bed dryer of mate leaves, Chem. Eng. Process. 46 (2007) 1365-1375.
[25] R. Amiri Chayjan, M. Kaveh, Physical parameters and kinetic modeling of fix and fluid bed drying of terebinth seeds, J. Food Process. Pres. 38 (2014) 1307-1320.
[26] S. Aral, A.V. Beşe, Convective drying of hawthorn fruit (Crataegus spp.): Effect of experimental parameters on drying kinetics, color, shrinkage, and rehydration capacity, Food Chem. 210 (2016) 577-584.
[27] S. Mercier, S. Villeneuve, M. Mondor, L.-P. Des Marchais, Evolution of porosity, shrinkage and density of pasta fortified with pea protein concentrate during drying, LWT-Food Sci. Technol. 44 (2011) 883-890.
[28] İ. Doymaz, Convective drying kinetics of strawberry, Chem. Eng. Process. 47 (2008) 914-919.
[29] C. Hii, C. Law, M. Cloke, Modeling using a new thin layer drying model and product quality of cocoa, J. Food Eng. 90 (2009) 191-198.
[30] C. Ertekin, O. Yaldiz, Drying of eggplant and selection of a suitable thin layer drying model, J. Food Eng. 63 (2004) 349-359.
[31] H.O. Menges, C. Ertekin, Thin layer drying model for treated and untreated Stanley plums, Energ. Convers. Manage. 47 (2006) 2337-2348.
[32] O. Molerus, K.-E. Wirth, Heat transfer in fluidized beds, Vol. 11, Springer Science & Business Media, 2012.
[33] F. Göğüş, M. Maskan, Air drying characteristics of solid waste (pomace) of olive oil processing, J. Food Eng. 72 (2006) 378-382.
[34] I. Doymaz, O. Gorel, N.A. Akgun, Drying Characteristics of the Solid By-product of Olive Oil Extraction, Biosyst. Eng. 88 (2004) 213-219.
[35] N.A. Akgun, I. Doymaz, Modelling of olive cake thin-layer drying process, J. Food Eng. 68 (2005) 455-461.
[36] K. Sacilik, R. Keskin, A.K. Elicin, Mathematical modelling of solar tunnel drying of thin layer organic tomato, J. Food Eng. 73 (2006) 231-238.
[37] E.K. Akpinar, Y. Bicer, Mathematical modelling of thin layer drying process of long green pepper in solar dryer and under open sun, Energ. Convers. Manage. 49 (2008) 1367-1375.
[38] S.J. Babalis, V.G. Belessiotis, Influence of the drying conditions on the drying constants and moisture diffusivity during the thin-layer drying of figs, J. Food Eng. 65 (2004) 449-458.